

Maltose–neopentyl glycol (MNG) amphiphiles for solubilization, stabilization and crystallization of membrane proteins

Pil Seok Chae¹, Søren G F Rasmussen², Rohini R Rana³, Kamil Gotfryd⁴, Richa Chandra⁵, Michael A Goren⁶, Andrew C Kruse², Shailika Nurva⁵, Claus J Loland⁴, Yves Pierre⁷, David Drew³, Jean-Luc Popot⁷, Daniel Picot⁷, Brian G Fox^{6,8}, Lan Guan⁵, Ulrik Gether⁴, Bernadette Byrne³, Brian Kobilka² & Samuel H Gellman¹

The understanding of integral membrane protein (IMP) structure and function is hampered by the difficulty of handling these proteins. Aqueous solubilization, necessary for many types of biophysical analysis, generally requires a detergent to shield the large lipophilic surfaces of native IMPs. Many proteins remain difficult to study owing to a lack of suitable detergents. We introduce a class of amphiphiles, each built around a central quaternary carbon atom derived from neopentyl glycol, with hydrophilic groups derived from maltose. Representatives of this maltose–neopentyl glycol (MNG) amphiphile family show favorable behavior relative to conventional detergents, as manifested in multiple membrane protein systems, leading to enhanced structural stability and successful crystallization. MNG amphiphiles are promising tools for membrane protein science because of the ease with which they may be prepared and the facility with which their structures may be varied.

Integral membrane proteins (IMPs) play crucial roles in many aspects of biology by mediating the transfer of material and signals between cells and their environment. It is estimated that 20–30% of all open reading frames in the human genome encode membrane proteins and that more than 50% of current pharmaceutical agents target IMPs¹. Our understanding of IMP structure and function, however, is hampered by difficulties associated with handling these proteins². Most IMPs are not soluble in aqueous buffer because they have large hydrophobic surfaces when properly folded; therefore, detergents are required to extract IMPs from the lipid bilayer and to maintain their native states in solution. Mild detergents are widely used for IMP manipulation, but many membrane proteins tend to denature and/or aggregate when

solubilized with these agents³, making it difficult to conduct functional studies, spectroscopic analysis or crystallization trials.

Earlier efforts to develop amphiphiles tailored for IMP applications have involved diverse strategies and achieved varying levels of success. Several peptide-based designs have been explored (peptidetergents⁴, lipopeptide detergents⁵, short peptide surfactants⁶) but so far have not gained broad acceptance. Amphiphilic polymers (“amphipols”^{7,8}) and discoidal lipid bilayers stabilized by an amphiphilic protein scaffold (“nanodiscs”^{9,10}) have proven to be versatile tools for studying IMPs in native-like states in aqueous solution. It is not clear, however, whether either of these approaches can yield high-quality crystals for diffraction analysis, a prominent objective of IMP studies. Furthermore, neither amphipols nor nanodiscs are designed to extract IMPs from biological membranes. Recently reported agents of low molecular weight, such as hemifluorinated surfactants (HFS)^{8,11} and cholic acid–based amphiphiles¹², have shown promising properties, but the scope of their utility remains to be explored. Thus there has been a need for amphiphiles that can extract, stabilize and promote crystallization of IMPs more effectively than do current detergents. Amphiphiles with this combination of capabilities would have to be easily prepared on a large scale, which would be extremely challenging for peptide- or protein-based agents.

Here we report a class of amphiphiles that show favorable behavior with a diverse set of membrane proteins. The design of these amphiphiles features a central quaternary carbon, which is intended to place subtle restraints on conformational flexibility^{13–15}. Because the quaternary carbon was derived from neopentyl glycol and because the hydrophilic groups in the examples discussed here are derived from maltose, we designate these compounds maltose–neopentyl glycol (MNG) amphiphiles. The quaternary

¹Department of Chemistry, University of Wisconsin–Madison, Madison, Wisconsin, USA. ²Molecular and Cellular Physiology, Stanford University, Stanford, California, USA. ³Division of Molecular Biosciences, Department of Life Sciences, Imperial College London, London, UK. ⁴Molecular Neuropharmacology Group, Department of Neuroscience and Pharmacology, Faculty of Health Sciences, University of Copenhagen, Copenhagen, Denmark. ⁵Department of Cell Physiology and Molecular Biophysics, Center for Membrane Protein Research, Texas Tech University Health Sciences Center, Lubbock, Texas, USA. ⁶Department of Biochemistry, University of Wisconsin–Madison, Madison, Wisconsin, USA. ⁷Laboratoire de Biologie Physico-Chimique des Protéines Membranaires, Centre National de la Recherche Scientifique/Université Paris-7 Unité Mixte de Recherche 7099, Institut de Biologie Physico-Chimique, Paris, France. ⁸Center for Eukaryotic Structural Genomics, University of Wisconsin–Madison, Madison, Wisconsin, USA. Correspondence should be addressed to S.H.G. (gellman@chem.wisc.edu), B.K. (kobilka@stanford.edu) or B.B. (b.byrne@imperial.ac.uk).

carbon distinguishes MNG architecture from conventional detergent structures and enables the incorporation of two hydrophilic and two lipophilic subunits. We hypothesized that the modulation of flexibility and distinctive orientations of hydrophilic and lipophilic surfaces would give MNG amphiphiles properties distinct from those of analogous conventional detergents. These amphiphiles are readily synthesized. We have evaluated their performance with multiple membrane proteins in diverse applications, including maintenance of native IMP folding, association and function, extraction from a native membrane, growth of high-quality crystals and support of cell-free translation.

RESULTS

MNG amphiphile architecture

We performed extensive preliminary studies that identified MNG-1, MNG-2 and MNG-3 (Fig. 1) as showing particularly promising behavior. Each of these amphiphiles features two maltose units in its hydrophilic portion and two *n*-decyl chains in its lipophilic portion. The lipophilic unit attachment varies, with amide linkages in MNG-1, ether linkages in MNG-2 and direct connection to the quaternary center in MNG-3. Synthesis of each compound was straightforward and efficient (Supplementary Note). We prepared analogs with conventional detergent architecture, MPA-1 to MPA-4 (for monopodal amphiphile), for comparison with MNG-1 and MNG-2 (Fig. 1). The comparison compounds for MNG-3 are commercially available—*n*-undecyl- β -D-maltoside (UDM) and *n*-dodecyl- β -D-maltoside (DDM, currently one of the most widely used detergents in membrane protein research); we also examined the lower homolog decyl- β -D-maltoside (DM) and the higher homolog tridecyl- β -D-maltoside (TDM), both of which are commercially available as well.

MNG amphiphiles stabilize diverse membrane proteins

We first examined the thermal stability of a human β_2 adrenergic receptor-T4 lysozyme fusion protein (β_2 AR-T4L)¹⁶ solubilized with an MNG amphiphile or conventional detergent. Stability was assessed via optical absorption measurements of β_2 AR-T4L bound to the inverse agonist carazolol (fluorescence emission maximum at 341 nm in the receptor-bound state and at 356 nm after carazolol release from the receptor). The receptor was initially solubilized and purified with DDM, which was then exchanged for the amphiphile or detergent to be evaluated. The 341 nm/356 nm peak-intensity ratio was used to monitor the relative amounts of intact and denatured β_2 AR-T4L (Supplementary Fig. 1). We evaluated the effect of amphiphile concentration on the melting temperature (T_m) of β_2 AR-T4L (Supplementary Fig. 2 and Supplementary Table 1). All three MNG amphiphiles were superior to DDM and other conventional detergents (including DM and TDM) in their effects on β_2 AR-T4L thermal stability (Fig. 2a). The concentration ranges that confer optimal stabilization in each case were similar in terms of weight percentage (between 0.05 and 0.1 wt %) but differed somewhat on a scale based on

critical micelle concentration (CMC) (Supplementary Fig. 2b). The most successful amphiphile was MNG-3. MNG-3 was superior to DDM as well in terms of maintaining a solubilized form of the muscarinic M_3 acetylcholine receptor (M_3 AchR) in an active state (Fig. 2b). Together, the observations with β_2 AR-T4L and M_3 AchR raised the possibility that MNG amphiphiles will be generally useful for G protein-coupled receptor (GPCR) stabilization.

We turned next to melibiose permease (MelB), which catalyzes the accumulation of α -D-galactopyranosides by a cation-solute symport mechanism¹⁷. Treatment of membrane preparations containing overexpressed MelB (from *Escherichia coli* DW2 cells) with solutions containing 1.5 wt % amphiphile or detergent at 0 °C for 10 min quantitatively extracted MelB (Fig. 3). To assess protein thermostability, we incubated the solubilized samples on ice or at elevated temperatures for 90 min before ultracentrifugation. For the conventional detergents (MPA-1, MPA-3 and DDM), we observed MelB aggregation when the protein was incubated at 45 °C for 90 min, and the protein disappeared from solution when subjected to treatment at 55 °C or 65 °C followed by ultracentrifugation (Fig. 3). In contrast, all three MNG amphiphiles provided large amounts of soluble protein even after treatment at 55 °C. In particular, MNG-3 was unique in preventing aggregation at 55 °C.

We assessed the thermostabilities of additional membrane protein systems via a fluorescence assay. *N*-[4-(7-Diethylamino-4-methyl-3-coumarinyl)phenyl]maleimide (CPM)¹⁸ can be selectively and covalently attached to side chain thiol groups of solvent-accessible cysteine residues. The maleimide unit of CPM quenches coumarin fluorescence; however, the coumarin unit becomes fluorescent after the maleimide reacts with a thiol. This assay provides insight on unfolding for membrane proteins that have buried cysteine residues in the native conformation, because cysteine side chains that become exposed as a result of unfolding are reactive. We applied the CPM assay to two prokaryotic respiratory complexes, succinate:quinone oxidoreductase (SQR)¹⁹ and cytochrome *bo*₃ ubiquinol oxidase (cytochrome *bo*₃)²⁰ from *E. coli*, and to the mouse cytidine-5'-monophosphate-sialic acid transporter (CMP-Sia)²¹. SQR was purified with the conventional detergent C12E9, and cytochrome *bo*₃ and CMP-Sia were purified with DDM. The purified membrane protein-detergent preparations were individually diluted into solutions containing an amphiphile at 10 \times CMC, and the unfolding in each protein sample was monitored over time at

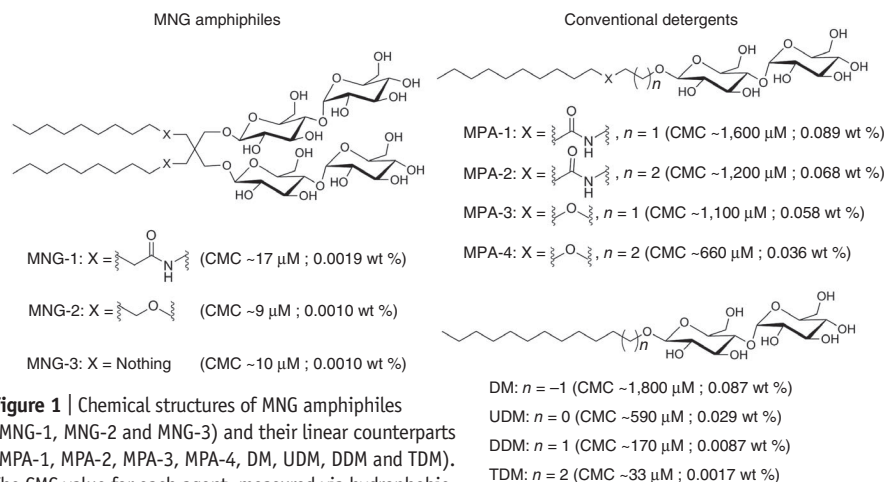


Figure 1 | Chemical structures of MNG amphiphiles (MNG-1, MNG-2 and MNG-3) and their linear counterparts (MPA-1, MPA-2, MPA-3, MPA-4, DM, UDM, DDM and TDM). The CMC value for each agent, measured via hydrophobic dye solubilization, is indicated in parentheses.

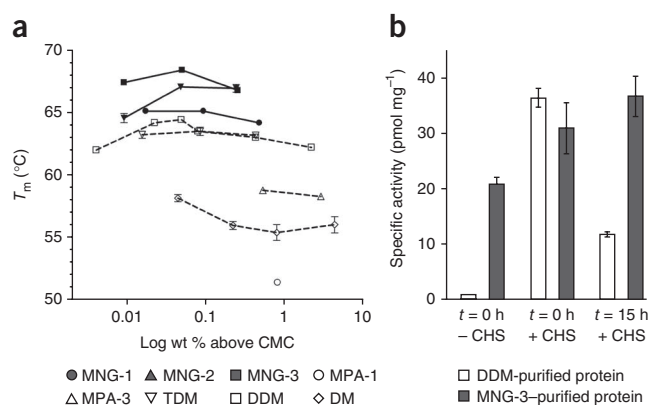


Figure 2 | GPCR stability in MNG amphiphiles or conventional detergents. (a) T_m values of β_2 AR-T4L plotted in terms of wt % of the MNG amphiphiles (MNG-1, MNG-2 and MNG-3) or conventional detergents (MPA-1, MPA-3, DM, DDM and TDM). β_2 AR-T4L with bound carazolol (an inverse agonist) was incubated with various agents at the various concentrations at indicated temperatures for 5 min before fluorescence emission measurements. Normalized results are expressed as mean \pm s.e.m. ($n = 3, 4$ or 5). (b) Specific activities (pmol mg^{-1}) of M_3 AchR in DDM and MNG-3. The activity of the protein was evaluated after the protein was washed and eluted with buffer including DDM or MNG-3, but without CHS, via a binding assay involving the antagonist [^3H]N-methylscopolamine, in the absence ($t = 0$ h, - CHS; first bar) or presence of CHS ($t = 0$ h, + CHS; second bar). The DDM- and MNG-3-purified M_3 AchR samples were stored at 4°C for 15 h, and then activities were measured again in the presence of CHS ($t = 15$ h, + CHS; third bar). Results are expressed as mean \pm s.d. ($n = 3$).

40°C . In addition to DDM, we evaluated MPA-4, DM and sodium dodecyl sulfate (SDS). SDS is widely recognized to be highly disruptive of native protein conformations, and this detergent caused the most rapid and extensive unfolding of each protein among the agents we examined (Fig. 4a and Supplementary Fig. 3). For each protein, the level of fluorescence observed with SDS after 130 min at 40°C was taken to indicate a limiting denatured state, and a lack of fluorescence was taken to indicate a native state.

All three MNG amphiphiles appeared to be superior to conventional detergents at maintaining native protein structure, as indicated by CPM assay results for SQR (Fig. 4a) and comparable results for cytochrome bo_3 and CMP-Sia (Supplementary Fig. 3a,b). DDM and MPA-4 were nearly as effective as the MNG amphiphiles, but DM was noticeably inferior. We next used gel filtration analysis to determine whether MNG-3 or DDM could maintain quaternary interactions among the four SQR subunits. After 120 min at 40°C in the presence of $10\times$ CMC DDM, the native quaternary structure of SQR was almost completely destroyed (Fig. 4b). In contrast, the quaternary structure remained largely intact after 130 min at 40°C in the presence of $10\times$ CMC MNG-3 (Fig. 4c). We also compared MNG-3 and DDM in an SQR functional assay. SQR must be thermally activated (by incubation at 30°C for 20 min) to remove bound oxaloacetate from the active site before assay. We incubated activated SQR with either MNG-3 or DDM at 40°C and then measured the catalytic efficacy of the protein (k_{cat}) immediately after activation (0 min) and at 60-min intervals thereafter. Both MNG-3 and DDM gave fairly high initial k_{cat} values, but SQR activity steadily declined with DDM, whereas activity was maintained or even slightly improved with MNG-3 (Fig. 4d). Overall, these results show that MNG-3 maintains the SQR quaternary assembly in a fully native state and that the MNG amphiphile is superior to DDM in stabilizing catalytically competent SQR.

We turned to the bacterial leucine transporter (LeuT)²² to evaluate protein stability as a function of time at room temperature (rather than as an ability to resist thermal denaturation). LeuT, a bacterial member of the neurotransmitter:sodium symporter

family (NSS family) proteins²³, was solubilized and purified with DDM and then transferred into individual amphiphile solutions. We assessed LeuT activity in terms of its ability to bind [^3H]leucine via scintillation proximity assay²⁴. Preliminary studies, conducted at $10\times$ CMC, indicated that LeuT solubilized with several conventional detergents showed a rapid decline in activity, whereas LeuT solubilized with DDM showed a more gradual loss of activity; all three MNG amphiphiles were superior to DDM in terms of maintaining LeuT activity over time (Supplementary Fig. 4a,b). We conducted further studies involving the MNG amphiphiles and DDM with each agent at 0.026 wt % above its CMC (Fig. 5a and Supplementary Fig. 4c). Under these conditions, each MNG amphiphile kept LeuT fully soluble and fully active over the 12-d study period. In contrast, LeuT activity declined to $\sim 65\%$ after 12 d in the presence of DDM (Fig. 5a).

MNG amphiphiles extract IMPs from native membranes

To assess the ability of MNG amphiphiles to extract intrinsic proteins from their native membranes, we examined the photosynthetic superassembly of *Rhodobacter capsulatus*²⁵. These studies used membranes isolated from an *R. capsulatus* strain that lacks light-harvesting complex II (LHII)²⁶; in this case the

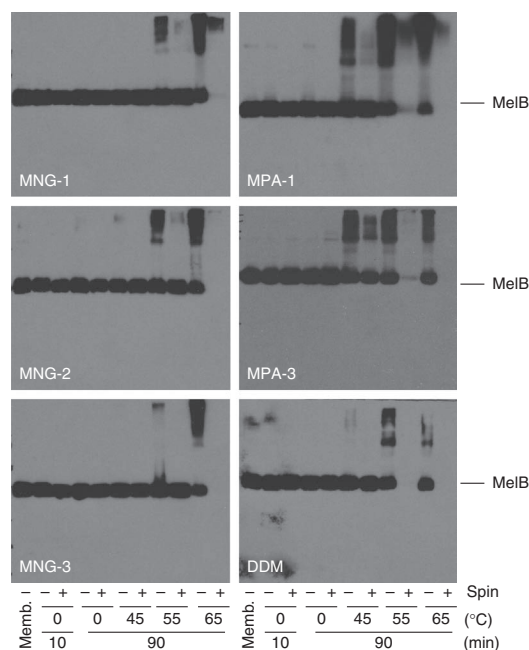


Figure 3 | SDS-12% PAGE analysis and western blot detection of MelB. MelB samples were subjected to SDS-PAGE analysis, and MelB was detected by western blotting using anti-histidine tag antibody. Each sample contained $10\ \mu\text{g}$ membrane proteins. For extracts generated with each detergent or amphiphile, one sample was subjected to ultracentrifugation (+) and a comparison sample was not (-). As a control, an untreated membrane sample (no ultracentrifugation) was included in each gel.

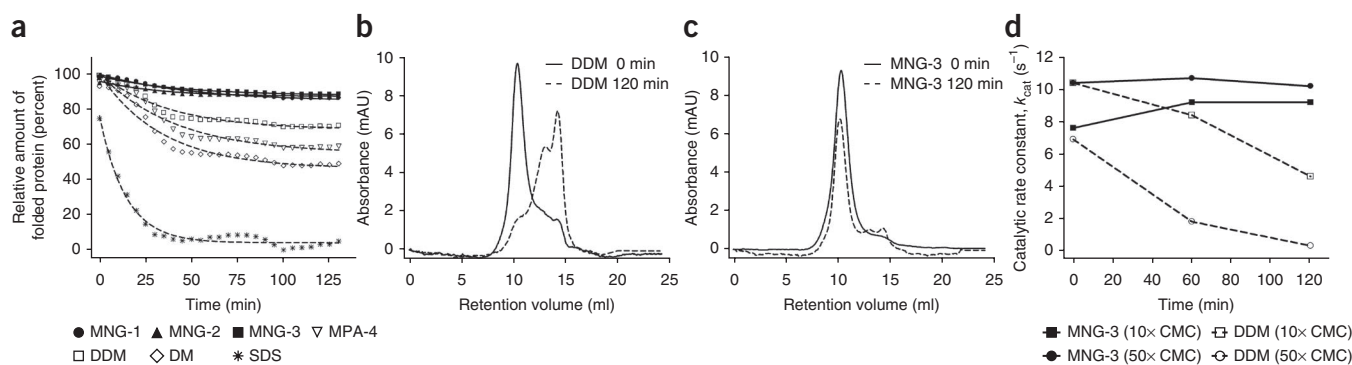


Figure 4 | Stability of SQR solubilized with MNG amphiphiles or conventional detergents. **(a)** Results of CPM assays for SQR solubilized with MNG amphiphiles (MNG-1, MNG-2 and MNG-3) or conventional detergents (MPA-4, DDM, DM and SDS) at 10 \times CMC. The unfolding of each protein was monitored at 40 $^{\circ}$ C for 130 min using a microplate spectrofluorometer. **(b,c)** Gel filtration analysis of SQR in DDM **(b)** or MNG-3 **(c)** at 10 \times CMC. SQR in DDM or MNG-3 was incubated for 120 min at 40 $^{\circ}$ C (AU, absorbance unit). **(d)** Time course of SQR activity in MNG-3 or DDM. Each agent was used at 10 \times CMC (0.01 wt % for MNG-3, 0.087 wt % for DDM) and 50 \times CMC (0.05 wt % for MNG-3, 0.44 wt % for DDM). Note that 50 \times CMC MNG-3 is comparable to DDM at 10 \times CMC in terms of wt %. The catalytic rate constant (k_{cat}) is plotted as a function of incubation time. Data at $t = 0$ correspond to the activity of SQR following thermal activation performed at 30 $^{\circ}$ C for 20 min. Protein solubilized with each agent was incubated at 40 $^{\circ}$ C for a further 120 min, and activity of the protein was measured at the designated times. The k_{cat} values at each time point were calculated by analyzing reaction data according to Michaelis-Menten kinetics.

supraassembly comprises the very labile light-harvesting complex I (LHI) and the more resilient reaction-center complex (RC). This system is well suited for assessing extraction and stabilization properties of detergents and amphiphiles because the supraassembly can be detected and its composition can be qualitatively monitored via optical measurements¹⁵: intact LHI-RC supraassembly has a strong absorbance at 875 nm and a 875 nm/760 nm absorption ratio >7. (Absorbance at 760 nm arises from bacteriochlorophyll units that have dissociated from LHI.) We treated intracytoplasmic *R. capsulatus* membranes enriched in LHI-RC complex with solutions containing 1 wt % detergent or amphiphile for 30 min at 32 $^{\circ}$ C. MNG-2 and MNG-3 were effective at extracting the intact supraassembly (strong absorption at 875 nm; 875 nm/760 nm ratio ~9–10; **Supplementary Fig. 5**). Comparable efficacy was observed with MPA-3 and DDM (875 nm/760 nm ratio ~8.5), but other conventional detergents were less successful. After purification of solubilized samples (**Supplementary Fig. 6**), we monitored the supraassembly stability over time at room temperature based on the 875 nm/680 nm absorbance ratio (absorbance at 680 nm arises from oxidation of bacteriochlorophyll that has been released from LHI). We compared the three MNG amphiphiles to conventional detergents (DDM and MPA-3), with each agent at its CMC (**Fig. 5b**; comparisons involving other concentrations may be found in **Supplementary Fig. 7**). For all samples, the

875 nm/680 nm absorbance ratio declined over 20 d; however, at every time point, the ratio was higher for the samples solubilized with an MNG amphiphile than for the samples solubilized with a conventional detergent. Overall, the results with *R. capsulatus* photosynthetic proteins show that MNG amphiphiles can extract a protein quaternary structure intact from its native membrane and then provide superior structural stability over time relative to DDM or other conventional detergents.

We performed additional studies to evaluate the use of MNG-3 for extraction of other proteins from membranes. MNG-3 was comparable to the conventional detergents DDM and TDM, at 1 wt % or 2 wt %, for the extraction of wild-type β_2 AR from Sf9 insect cell membranes. We evaluated the activity of β_2 AR receptor via a binding assay with antagonist [³H]dihydroalprenolol (**Supplementary Fig. 8a**). At 1 wt %, MNG-3 was comparable to DDM and slightly inferior to TDM in terms of β_2 AR activity, but at 2 wt %, MNG-3 was superior to both conventional detergents. MNG-3 at 2 wt % yielded a receptor activity comparable to that of 1 wt % TDM. For extraction of LeuT from the bacterial membrane, MNG-3 proved to be somewhat inferior to DDM, providing only ~60% of the yield obtained with DDM. However, MNG-3-purified protein showed substrate affinity identical to that of DDM-purified protein (**Supplementary Fig. 8b**). For extraction of a CMP-Sia fusion protein bearing

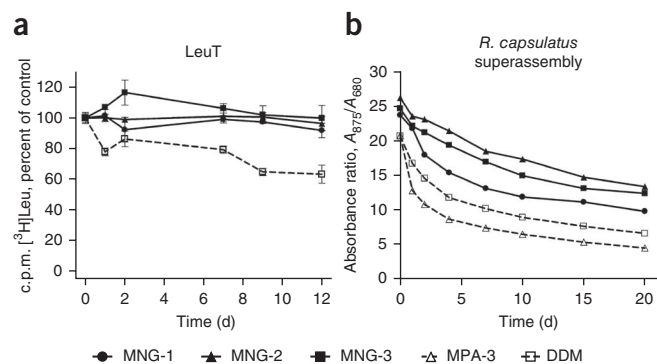
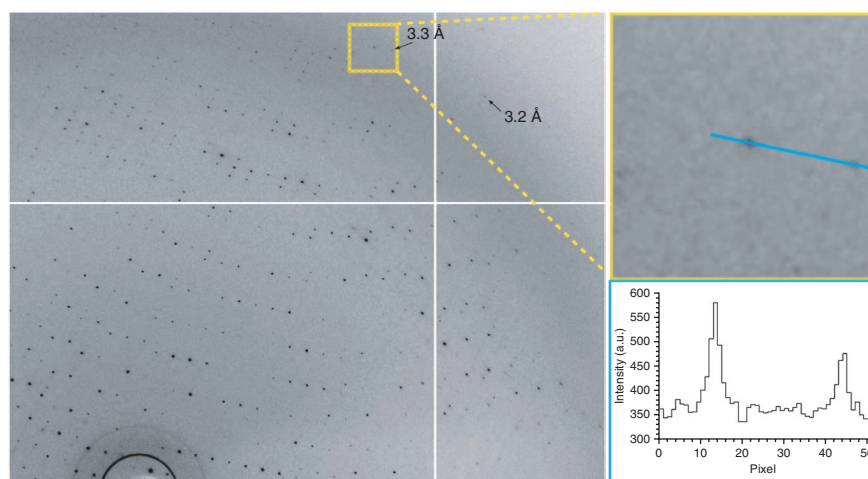


Figure 5 | Long-term stability of LeuT and *R. capsulatus* supraassembly in MNG amphiphiles or conventional detergents. **(a)** Time course of activity ([³H]leucine binding) assay for LeuT solubilized with MNG amphiphiles (MNG-1, MNG-2 and MNG-3) and DDM at 0.026 wt % above the critical micelle concentration (CMC) (total concentrations: 0.035 wt % DDM, 0.028 wt % MNG-1, 0.027 wt % MNG-2 and 0.027 wt % MNG-3). LeuT activity was monitored at indicated time points, using a scintillation proximity assay (SPA), for protein stored at the room temperature. Results are expressed as % activity relative to the appropriate day 0 measurement. Normalized results are expressed as mean \pm s.e.m. ($n = 2$). **(b)** Time course of stability of *R. capsulatus* supraassembly purified with MNG amphiphiles (MNG-1, MNG-2 and MNG-3) or conventional detergents (MPA-3 and DDM) at 1 \times CMC. The absorbance ratios (A_{875}/A_{680}) of the detergent or amphiphile samples were followed as a function of time.

Figure 6 | Image and X-ray diffraction pattern from crystals of cytochrome b_6f -MNG-3 complexes. X-ray diffraction by a cytochrome b_6f crystal obtained in the presence of MNG-3. Left panel represents a portion of the pattern (0.5° oscillation range). Resolution limits are marked with arrows (the white cross is due to the tiling of the detector). Top right, enlargement of the yellow square with two strong spots near the resolution limit. A section through the two strong spots is shown in the lower right corner (a.u., arbitrary unit).



green fluorescent protein (GFP) at the C terminus, expressed in *Saccharomyces cerevisiae*, MNG-3 and DDM provided comparable protein yields (70–80%); in each case, the protein was intact and homogenous (**Supplementary Fig. 8c**).

Overall, based on results from several different systems, MNG-3 appears to be comparable to DDM for extraction of membrane proteins from biological membranes.

We observed that MNG amphiphiles enabled the expression and concomitant solubilization of a membrane protein, bacterioopsin (BO), from a cell-free wheat germ-based translation system (**Supplementary Fig. 9**). DDM and other conventional detergents could solubilize only limited amounts of translated BO at 0.1 wt %, and these detergents inhibited cell-free translation at 0.2 wt %. In contrast, 0.2 wt % MNG-2 or MNG-3 was compatible with translation and solubilized most of the BO.

MNG amphiphiles aid in membrane protein crystallization

Growth of high-quality crystals that allow structure determination is one of the most important and challenging goals of membrane protein research. We examined crystallization of the cytochrome b_6f complex from *Chlamydomonas reinhardtii* with MNG-3. This protein assembly tends to denature in the presence of most conventional detergents, but DDM can maintain the native structure and has previously enabled crystallization and structure determination of the complex via X-ray diffraction²⁷. Cytochrome b_6f crystallization requires 0.2 mM DDM (CMC = 0.17 mM); lower detergent concentrations promote protein aggregation, whereas higher detergent concentrations lead to dissociation of subunits. We found that cytochrome b_6f in the presence of 0.5 mM MNG-3 showed stability comparable to that observed in the presence of 0.2 mM DDM. The tolerance for higher concentrations of MNG-3 relative to DDM provided a larger concentration window in which to attempt crystallization of solubilized cytochrome b_6f . Protein-containing crystals appeared within 24 h of setting up drops. After a few days, crystals reached a maximum size of $70 \times 400 \mu\text{m}$ (data not shown).

The diffraction data from cytochrome b_6f crystals grown with MNG-3 extended up to $\sim 3.4\text{-}\text{\AA}$ resolution (**Fig. 6** and **Supplementary Table 2**), a value similar to that commonly obtained for crystals grown with DDM. With DDM, extensive screening yielded crystals diffracting to 2.8\AA ²⁷. Fourier difference maps (of crystals with DDM²⁷ versus crystals with MNG-3) showed no notable features in the protein region (data not shown). However, substantial differences (up to 6.8σ) were observed in regions where detergent molecules have been localized in the crystals grown with DDM. These differences indicate that during the exchange of detergents, MNG-3 was able to displace the most

strongly bound DDM molecules. Further analysis by refinement of the protein structure starting from the DDM structure confirmed that the electron density of two DDM molecules had vanished and that a new molecule with a slightly different maltoside headgroup position, presumably MNG-3, occupied this position. This electron density, however, was not sufficiently well defined to allow model building of MNG-3, despite otherwise good refinement statistics for the protein (**Supplementary Table 2**).

Membrane protein crystallization from a lipidic cubic phase (LCP) is an increasingly popular strategy²⁸ that has, notably, led to the recent structure solution of $\beta_2\text{AR-T4L}$ ^{16,29,30}. We evaluated the ability of MNG-3 to promote LCP-based crystallization of two new forms of this GPCR, a fusion protein with a covalently attached agonist (unpublished data) and an agonist-bound $\beta_2\text{AR-T4L}$ stabilized by an antibody in an active state (unpublished data). Although efforts to crystallize DDM-solubilized agonist-bound receptor from a monoolein-water LCP yielded crystals (data not shown), it was impossible to grow them large enough to obtain high-resolution diffraction. By contrast, in both cases detergent exchange into MNG-3 facilitated incorporation into the LCP, from which larger crystals suitable for X-ray diffraction analysis were obtained (data not shown). In the latter case, the crystals were $\sim 40 \times 5 \times 5 \mu\text{m}$, and X-ray diffraction data allowed solution of the structure to $3.5\text{-}\text{\AA}$ resolution. We speculate that the enhanced stability of $\beta_2\text{AR-T4L}$ solubilized by MNG-3 relative to the DDM-solubilized form may be crucial for successful transfer of the protein into the LCP.

DISCUSSION

Our results suggest that MNG amphiphiles will be generally useful for membrane protein biochemistry research. MNG amphiphiles can be readily prepared in multi-gram quantities, and this synthetic accessibility should enable their evaluation with many systems, including efforts directed toward structural analysis (for example, through nuclear magnetic resonance spectroscopy³¹ or mass spectrometry³²) and the incorporation of MNG amphiphiles into new techniques for membrane protein purification and manipulation³³. Given the diversity of shapes, sequences and properties of membrane proteins and their assemblies, it seems very unlikely that any single amphiphile will be ideal for all or even a large subset of membrane proteins. The ease with which MNG amphiphile structure may be varied should facilitate the development of a suite of agents that, collectively, have broad utility.

Many important questions remain to be addressed in subsequent studies. For example, it will be valuable to assess the sizes of micelles formed by MNG amphiphiles and how micelle size is affected by changes in amphiphile structure. In addition, it will be useful to determine average numbers of amphiphile molecules per micelle. But even before these properties are elucidated, we anticipate, based on this first characterization study, that the MNG amphiphiles will become useful tools for membrane protein manipulation.

METHODS

Methods and any associated references are available in the online version of the paper at <http://www.nature.com/naturemethods/>.

Note: Supplementary information is available on the Nature Methods website.

ACKNOWLEDGMENTS

This work was supported by US National Institutes of Health (NIH) grant P01 GM75913 (S.H.G.), NS28471 (B.K.), by the Lundbeck Foundation (S.G.F.R., C.J.L. and U.G.), by the Danish National Research Council (C.J.L., U.G.), by the European Community's Seventh Framework Programme FP7/2007-2013 under grant agreement no. HEALTH-F4-2007-201924, EDICT Consortium (K.G., U.G. and B.B.) and by NIH grant GM083118 and NIH Protein Structure Initiative grants U54 GM-074901 (J.L. Markley, PI; B.G.F.) and U54 GM094584 (B.G.F.). This work was also supported by grant no. R21HL087895 from the US National Heart, Lung, and Blood Institute, by the Texas Norman Hackerman Advanced Research Program under grant no. 010674-0034-2009 (to L.G.) and by the Center for Membrane Protein Research, Texas Tech University Health Sciences Center. R.R.R. was funded by the Defence Science and Technology Laboratory. We thank P. Laible (Argonne National Laboratory, Chicago) for supplying membrane preparations from *R. capsulatus*. We acknowledge SOLEIL (Saint-Aubin, France) for provision of synchrotron radiation facilities, and we would like to thank B. Guimaraes for assistance in using the beamline Proxima 1. We also thank R. Kaback (University of California, Los Angeles) and G. Leblanc (Institut de Biologie et Technologies-Saclay) for the MelB expression system. M.A.G. acknowledges support from the US National Science Foundation East Asia and Pacific Summer Institutes Fellowship program. We thank G. Cecchini (University of California, San Francisco) and J. Ruprecht (Medical Research Council Mitochondrial Biology Unit, Cambridge) for the purified SQR and the details of the SQR functional assay, and we acknowledge the assistance of P. Nixon in the analysis of the SQR functional data.

AUTHOR CONTRIBUTIONS

P.S.C. designed the MNG amphiphiles, with contributions from S.G.F.R., B.K. and S.H.G. P.S.C. synthesized the amphiphiles. P.S.C., S.G.F.R., R.R.R., K.G., R.C., M.A.G., A.C.K., S.N., Y.P. and D.P. designed and performed the research and interpreted the data. C.J.L., D.D., B.G.F., L.G., U.G., J.-L.P., B.B., B.K. and S.H.G. contributed to experimental design and data interpretation. P.S.C. and S.H.G. wrote the manuscript, with oversight from S.G.F.R., R.R.R., K.G., R.C., M.A.G., A.C.K., S.N., C.J.L., Y.P., D.D., J.-L.P., D.P., B.G.F., L.G., U.G., B.B. and B.K.

COMPETING FINANCIAL INTERESTS

The authors declare competing financial interests: details accompany the full-text HTML version of the paper at <http://www.nature.com/naturemethods/>.

Published online at <http://www.nature.com/naturemethods/>.

Reprints and permissions information is available online at <http://npg.nature.com/reprintsandpermissions/>.

- Liu, J. & Rost, B. Comparing function and structure between entire proteomes. *Protein Sci.* **10**, 1970–1979 (2001).
- Lacapère, J.J., Pebay-Peyroula, E., Neumann, J.M. & Etchebest, C. Determining membrane protein structures: still a challenge! *Trends Biochem. Sci.* **32**, 259–270 (2007).
- Privé, G.G. Detergents for the stabilization and crystallization of membrane proteins. *Methods* **41**, 388–397 (2007).
- Schafmeister, C.E., Meircke, L.J.W. & Stroud, R.M. Structure at 2.5 Å of a designed peptide that maintains solubility of membrane proteins. *Science* **262**, 734–738 (1993).
- McGregor, C.-L. *et al.* Lipopeptide detergents designed for the structural study of membrane protein. *Nat. Biotechnol.* **21**, 171–176 (2003).

- Zhao, X. *et al.* Designer short peptide surfactants stabilize G protein-coupled receptor bovine rhodopsin. *Proc. Natl. Acad. Sci. USA* **103**, 17707–17712 (2006).
- Tribet, C., Audebert, R. & Popot, J.-L. Amphipols: polymers that keep membrane proteins soluble in aqueous solutions. *Proc. Natl. Acad. Sci. USA* **93**, 15047–15050 (1996).
- Popot, J.-L. Amphipols, nanodiscs, and fluorinated surfactants: three non-conventional approaches to studying membrane proteins in aqueous solutions. *Annu. Rev. Biochem.* **79**, 737–775 (2010).
- Nath, A., Atkins, W.M. & Sligar, S.G. Applications of phospholipid bilayer nanodiscs in the study of membranes and membrane proteins. *Biochemistry* **46**, 2059–2069 (2007).
- Borch, J. & Hamann, T. The nanodisc: a novel tool for membrane protein studies. *Biol. Chem.* **390**, 805–814 (2009).
- Breyton, C. *et al.* Micellar and biochemical properties of (hemi)fluorinated surfactants are controlled by the size of the polar head. *Biophys. J.* **97**, 1077–1086 (2009).
- Zhang, Q. *et al.* Designing facial amphiphiles for the stabilization of integral membrane protein. *Angew. Chem. Int. Edn.* **119**, 7153–7155 (2007).
- Hoffmann, R.W. Flexible molecules with defined shape-conformational design. *Angew. Chem. Int. Edn. Engl.* **31**, 1124–1134 (1992).
- McQuade, D.T. *et al.* Rigid amphiphiles for membrane protein manipulation. *Angew. Chem. Int. Edn.* **39**, 758–761 (2000).
- Chae, P.S., Wander, M.J., Bowling, A.P., Laible, P.D. & Gellman, S.H. Glycotripod amphiphiles for solubilization and stabilization of a membrane protein superassembly: importance of branching in the hydrophilic portion. *ChemBioChem* **9**, 1706–1709 (2008).
- Rosenbaum, D.M. *et al.* GPCR engineering yields high-resolution structural insights into β_2 -adrenergic receptor function. *Science* **318**, 1266–1273 (2007).
- Bassilana, M., Pourcher, T. & Lablanc, G. Melibiose permease of *Escherichia coli*. *J. Biol. Chem.* **263**, 9663–9667 (1988).
- Alexandrov, A.I., Mileni, M., Chien, E.Y., Hanson, M.A. & Stevens, R.C. Microscale fluorescent thermal stability assay for membrane proteins. *Structure* **16**, 351–359 (2008).
- Horsefield, R., Iwata, S. & Byrne, B. Complex II from a structural perspective. *Curr. Protein Pept. Sci.* **5**, 107–118 (2004).
- Puustinen, A., Finel, M., Haltia, T., Gennis, R.B. & Wikström, M. Properties of the two terminal oxidases of *Escherichia coli*. *Biochemistry* **30**, 3936–3942 (1991).
- Newstead, S., Kim, H., von Heijne, G., Iwata, S. & Drew, D. High-throughput fluorescent-based optimization of eukaryotic membrane protein overexpression and purification in *Saccharomyces cerevisiae*. *Proc. Natl. Acad. Sci. USA* **104**, 13936–13941 (2007).
- Deckert, G. *et al.* The complete genome of the hyperthermophilic bacterium *Aquifex aeolicus*. *Nature* **392**, 353–358 (1998).
- Yamashita, A., Singh, S.K., Kawate, T., Jin, Y. & Gouaux, E. Crystal structure of a bacterial homologue of Na⁺/Cl⁻-dependent neurotransmitter transporters. *Nature* **437**, 215–223 (2005).
- Quick, M. & Javitch, J.A. Monitoring the function of membrane transport proteins in detergent-solubilized form. *Proc. Natl. Acad. Sci. USA* **104**, 3603–3608 (2007).
- Hu, X.C., Ritz, T., Damjanovic, A., Authenrieth, F. & Schulten, K. Photosynthetic apparatus of purple bacteria. *Q. Rev. Biophys.* **35**, 1–62 (2002).
- Youvan, D.C., Ismail, S. & Bylina, E.J. Chromosomal deletion and plasmid complementation of the photosynthetic reaction center and light-harvesting genes from *Rhodospseudomonas capsulata*. *Gene* **38**, 19–30 (1985).
- Stroebel, D., Choquet, Y., Popot, J.-L. & Picot, D. An atypical haem in the cytochrome *b₆f* complex. *Nature* **426**, 413–418 (2003).
- Rosenbaum, D.M., Rasmussen, S.G.F. & Kobilka, B.K. The structure and function of G-protein-coupled receptors. *Nature* **459**, 356–363 (2009).
- Cherezov, V. *et al.* High-resolution crystal structure of an engineered human β_2 -adrenergic G protein-coupled receptor. *Science* **318**, 1258–1265 (2007).
- Hanson, M.A. *et al.* A specific cholesterol binding site is established by the 2.8 Å structure of the human β_2 -adrenergic receptor. *Structure* **16**, 897–905 (2008).
- Sanders, C.R. & Sonnichsen, F. Solution NMR of membrane proteins: practice and challenges. *Magn. Reson. Chem.* **44**, S24–S40 (2006).
- Barrera, N.P., Di Bartolo, N., Booth, P.J. & Robinson, C.V. Micelles protect membrane complexes from solution to vacuum. *Science* **321**, 243–246 (2008).
- Li, L. *et al.* Simple host-guest chemistry to modulate the process of concentration and crystallization of membrane proteins by detergent capture in a microfluidic device. *J. Am. Chem. Soc.* **130**, 14324–14328 (2008).

ONLINE METHODS

Detergents and amphiphiles. We purchased conventional detergents (DM, UDM, DDM, TDM, LDAO, SDS and OG) from Anatrace. We obtained the starting materials and reagents used for preparation of MNG amphiphiles from Sigma-Aldrich. We used all of these agents without purification. Details of the syntheses of MNG amphiphiles can be found in the **Supplementary Note**.

β_2 AR stabilization and solubilization studies. The β_2 AR-T4L was expressed in Sf9 insect cells, solubilized and purified in DDM as previously described¹⁶. Briefly, the receptor was purified by M1 Flag antibody affinity chromatography before and after an alprenolol-Sepharose chromatography step. Carazolol was bound to the receptor on the second M1 resin after extensive washing in HEPES low-salt buffer (0.1% DDM, 100 mM NaCl, 20 mM HEPES, pH 7.5) containing 30 μ M carazolol. The eluted and carazolol-bound receptor was dialyzed against the same buffer containing 1 μ M carazolol to reduce free carazolol concentration. The β_2 AR-T4L was spin concentrated to 7 mg ml⁻¹ (~140 μ M) using a 100-kDa molecular-weight-cut-off (MWCO) Vivaspin concentrator (Vivascience). For stability measurements, the carazolol-bound receptor was diluted below the CMC for DDM by adding 3 μ l of the concentrated receptor in a quartz cuvette containing 600 μ l buffer (100 mM NaCl, 20 mM HEPES, pH 7.5) with detergents and amphiphiles at various concentrations ranging from 1.5 \times to 250 \times CMC. The cuvette was placed in a Spex FluoroMax-3 spectrofluorometer (Jobin Yvon Inc.) under Peltier temperature control. Fluorescence emission from carazolol was obtained after 5-min incubations from 25 $^{\circ}$ C to 85 $^{\circ}$ C in 12 successive 5 $^{\circ}$ C increments. Excitation was set at 325 nm, and emission was measured from 335 nm to 400 nm with an integration time of 0.3 s nm⁻¹ using a bandpass of 1 nm for both excitation and emission. The 341 nm/356 nm peak ratio was calculated and graphed using Microsoft Excel and GraphPad Prism software. For solubilization study from cell membranes, Sf9 cells were grown to a density of approximately 4 \times 10⁶ per ml and then infected with baculovirus expressing the wild-type β_2 AR (truncated after residue 365). After 48 h cells were harvested by centrifugation. No exogenous ligand was present during protein expression. Cells were resuspended, incubated in ice-cold lysis buffer (1 mM EDTA, 10 mM Tris, pH 8) containing protease inhibitors (5 μ g ml⁻¹ leupeptin and 320 μ g ml⁻¹ benzamidine) for 5 min and then pelleted by centrifugation (10 min, 4 $^{\circ}$ C, 16,000g). The pellet was resuspended in PBS saline and aliquoted into 1.5-ml tubes so that each tube contained 35 mg of wet pellet after centrifugation and removal of supernatant. Solubilization buffers contained 100 mM NaCl, 20 mM HEPES, pH 7.5, 5 μ g ml⁻¹ leupeptin, 320 μ g ml⁻¹ benzamidine, and either 1 wt % or 2 wt % of the indicated detergent. 300 μ l of solubilization buffer was added to each pellet, which was resuspended and homogenized by forcing the mixture through a 27-gauge syringe 30 times. Tubes were rocked at 4 $^{\circ}$ C for 1.5 h and then centrifuged at 16,000g to pellet insoluble material. The supernatant was then checked for total protein content by using a Bio-Rad D_C protein assay calibrated against a BSA standard. Measurements were performed in triplicate and then averaged. Active protein content was determined by incubating soluble material with the antagonist [³H]dihydroalprenolol at a single saturating concentration (10 nM) for 40 min and then separating bound from free

radioligand using a Sephadex G-50 column (GE Healthcare). All binding reactions were performed in buffer containing 0.1% of the same detergent used in solubilization, and G-50 columns were likewise equilibrated and eluted in this buffer (100 mM NaCl, 20 mM HEPES, pH 7.5, 0.1% detergent). Nonspecific binding was determined in the same manner but with the addition of 10 μ M alprenolol to the binding reaction. All binding reactions were performed in triplicate, and protein was diluted before binding such that bound radioligand never exceeded 10% of the total.

Muscarinic M₃ acetylcholine receptor activity assay. M₃ muscarinic acetylcholine receptor with the third intracellular loop replaced by T4 lysozyme and an N-terminal Flag epitope tag added was expressed in the same manner as described above, but with the addition of 1 μ M atropine to culture medium upon infection. Cells were lysed as described. Following centrifugation, the lysed cell pellet from 1 liter of culture was mixed with 200 ml M3 solubilization buffer (400 mM NaCl, 0.03% cholesterol hemisuccinate, 20 mM HEPES pH 7.5, 0.2% sodium cholate, 1% DDM, 5 μ g ml⁻¹ leupeptin, 320 μ g ml⁻¹ benzamidine). After being dounce homogenized 20 times with a tight pestle, the material was stirred at 4 $^{\circ}$ C for 1 h. 400 ml of dilution buffer containing 0.1% DDM, 20 mM HEPES pH 7.5, 30 mM NaCl, 3 mM CaCl₂, 5 μ g ml⁻¹ leupeptin and 320 μ g ml⁻¹ benzamidine was added with stirring, and the mix was then centrifuged to remove insoluble material. The resulting supernatant was split in half and flowed over Flag affinity columns to bind the protein. Protein was then washed with either 50 ml of high-salt DDM buffer (0.1% DDM, 20 mM HEPES pH 7.5, 500 mM NaCl, 0.01% CHS 5 μ g ml⁻¹ leupeptin, 320 μ g ml⁻¹ benzamidine) or exchanged into MNG-3 buffer (0.1% MNG-3, 20 mM HEPES, 500 mM NaCl, <0.01% CHS, 5 μ g ml⁻¹ leupeptin, 320 μ g ml⁻¹ benzamidine). The exchange was performed over the course of 1.5 h by increasing MNG-3 and decreasing DDM concentrations in 0.005% increments until the final 0.1% concentration of MNG-3 was reached. Columns were then washed with 50 ml of DDM buffer without CHS or with MNG-3 buffer without CHS (with MNG-3 decreased to 0.01%), over the course of 50 min. These and all other wash buffers contained 2 mM CaCl₂. Columns were eluted in washing buffer with 5 mM EDTA and no CaCl₂ with 0.2 mg ml⁻¹ Flag peptide added. Elution volumes for MNG-3 and DDM were identical. After elution, binding reactions were performed as described above but using a saturating concentration of [³H]N-methylscopolamine (10 nM). Nonspecific binding was measured in the presence of 10 μ M atropine. Protein assay was done as described above. All M3 binding reactions and G-50 elution with MNG-3 were performed at 0.01% concentration. Binding was measured again after overnight incubation at 4 $^{\circ}$ C.

MelB thermostability assay. Vector pK95 Δ AHB/WT MelB/CH₆, encoding the wild-type MelB with a hexahistidine (His₆) tag at the C terminus, and *E. coli* DW2-R cells (Δ melB and Δ lacZY) were gifts from G. Leblanc (Institut de Biologie et Technologies-Saclay). Overexpression of MelB was performed as described³⁴. Cells were harvested, resuspended in a buffer containing 20 mM Tris, pH 7.5, 200 mM NaCl and 10% glycerol, broken by French press and centrifuged at 20,000g for 15 min to remove unbroken cells. Membranes were then harvested from the supernatant by ultracentrifugation at 43,000 r.p.m. for 3 h in the Beckman Ti 45 rotor. The pellets

were resuspended in the same buffer, frozen in liquid N₂ and then stored at -80 °C until use. A protein assay was performed with a BCA kit (Thermo Scientific). For solubilization and thermostability assay, membrane samples containing MelB at a final protein concentration of 10 mg ml⁻¹ in a solubilization buffer (20 mM Tris, 200 mM NaCl, 10% glycerol, 20 mM melibiose, pH 7.5) were incubated with 1.5% (w/v) of a given amphiphile or detergent at 0 °C for 10 min and subsequently placed at a given temperature (0, 45, 55 or 65 °C) for 90 min. Samples were collected and then ultracentrifuged at 355,590g in a Beckman Optima™ MAX ultracentrifuge using a TLA-100 rotor for 45 min at 4 °C. 10 µg protein, from untreated membrane or detergent extracts, and equal volumes of the solutions after ultracentrifugation were analyzed by 12% SDS-PAGE and immunoblotted with pentahistidine antibody conjugated to horseradish peroxidase (His₅-HRP; Qiagen).

SQR, Cyt *bo*₃ and CMP-Sia thermostability assay and SQR size exclusion chromatography (SEC) analysis and functional assay.

The thermostability assay method was performed as described¹⁸ with the following minor modifications. CPM dye (Invitrogen), stored in DMSO (Sigma), was diluted in dye buffer (20 mM Tris (pH 7.5), 150 mM NaCl, 0.03% DDM, 5 mM EDTA). All the detergents were used at 10× CMC values in test buffer (20 mM Tris (pH 7.5), 150 mM NaCl). The test proteins—SQR, Cyt *bo*₃ and CMP-Sia (10 mg ml⁻¹)—were diluted (1:150) in test buffer in Greiner 96-well plates, and 3 µl of diluted CPM dye was added to each test condition. The reaction was monitored for 130 min at 40 °C using a microplate spectrofluorometer set at excitation and emission wavelengths of 387 nm and 463 nm, respectively. Relative maximum fluorescence was used to calculate percentage of relative folded protein remaining after 130 min at 40 °C. Relative unfolding profiles of proteins were plotted against time using GraphPad Prism. For SEC analysis, test protein samples of SQR were diluted (1:100) in SEC buffer (20 mM Tris (pH 7.5), 150 mM NaCl) containing either DDM or MNG-3 at 10× CMC. Aliquots (500 µl) of the diluted protein were either applied directly onto the column or heated at 40 °C for 120 min before being loaded onto a Superdex 200 column (GE Healthcare) pre-equilibrated in the respective SEC buffers. For the functional assay of SQR, DDM and MNG-3 at 10× or 50× CMC were used in activation and assay buffers. SQR was activated in buffer (30 mM K₂PO₄, 0.2 mM EDTA, 10 mM malonate) to remove bound oxaloacetate from the active site. The sample was diluted to 1 mg ml⁻¹ in activation buffer and then a further 50 times in the same buffer. Enzyme activation was performed at 30 °C for 20 min, aliquots were removed and then the samples were heated at 40 °C for 60 min and 120 min. The amount of functional SQR was estimated based on the succinate-Q1-DCIP reductase activity of the samples. Functional activity was monitored at 600 nm as a decrease of absorbance of 2,6-dichloroindophenol (DCIP) (extinction coefficient = 21.8 mM⁻¹ cm⁻¹) when 50 µM DCIP, 10 mM succinate, varied amounts of coenzyme Q1 (CoQ1) including blank and 0.6 µl of activated and/or heated SQR enzyme samples were added to assay buffers. The slopes of the absorbance curves (up to 20 min) were measured for a range of concentrations of CoQ1 (0 to 30 µM) and converted to initial velocity (*V*₀) values using the Beer-Lambert law. The *V*₀ values were plotted against CoQ1 concentrations for each detergent condition to fit the Michaelis-Menten equation. The saturation

concentration of CoQ1 was obtained for each condition as 20 µM. The Michaelis-Menten equation was used to calculate catalytic parameters for SQR-catalyzed succinate-Q1-DCIP reductase activity. The specific activity (*k*_{cat}) for SQR was calculated from 1-ml assay as follows. On addition of the enzyme, the change in absorbance over the initial 3 min of the reaction at 20 µM CoQ1 was converted to rate of the reaction using the Beer-Lambert law. Because this rate of the reaction at 20 µM CoQ1 is also the *V*_{max}, the *k*_{cat} values were calculated as rate per amount of enzyme.

CMP-Sia solubilization. Expression and solubilization of CMP-Sia was performed as described previously³⁵. In brief, the CMP-Sia was expressed as a fusion protein with a C-terminal GFP in FGY217 *Saccharomyces cerevisiae* cells. Membranes, generated as described previously³¹ were resuspended in 50 mM Tris-HCl (pH 7.5), 1 mM EDTA, 0.6 M sorbitol and the protein concentration measured. The membranes were adjusted to a concentration of 1 mg ml⁻¹ and 1-ml aliquots were solubilized individually in DDM and MNG-3 at final detergent concentrations of 0.5 wt %, 1.0 wt %, and 2.0 wt % for 1 h at 4 °C. 100-µl aliquots were removed from each tube, and a fluorescence reading was taken for each sample before and after ultracentrifugation at 150,000g for 1 h to remove insoluble material. The solubilization efficiency (%) is the fluorescence reading of the soluble supernatant divided by the fluorescence reading of the total sample times 100. The remaining soluble fraction for each condition was submitted to fluorescent SEC (FSEC) as described previously³⁶ using a Superose 6 column (GE Healthcare) equilibrated with buffer containing the appropriate agent (DDM or MNG-3).

LeuT solubilization, solubility and functionality assay. The wild-type version of the leucine transporter (LeuT) from *Aquifex aeolicus* in pET16b (pET16b-LeuT-His₈) was expressed in *Escherichia coli* essentially as described²². The plasmid was kindly provided by E. Gouaux (Vollum Institute, Portland, Oregon, USA). LeuT was purified from isolated cell membranes solubilized with 1% DDM and was then subjected to Ni²⁺-affinity chromatography using Chelating Sepharose Fast Flow (GE Healthcare) and elution in buffer composed of 20 mM Tris-HCl (pH 8.0), 1 mM NaCl, 199 mM KCl, 0.05% DDM and 300 mM imidazole. For comparison, in the solubilization assay, LeuT was extracted and eluted using MNG-3 in the final concentration of 1% and 0.042%, respectively. In the solubility and functionality assay, selected LeuT fractions eluted in the presence of 0.05% DDM were pooled, divided into aliquots and diluted in the above-mentioned buffer without DDM but containing MNG amphiphiles or conventional detergents to the final concentration of 10× CMC or 0.026 wt % above their CMC values (OG was tested at 2× CMC). After incubation at the room temperature, samples were centrifuged, and the protein concentration was determined at the indicated time points based on absorbance at 280 nm. Concomitantly, at the corresponding time points, [³H]leucine binding was assessed by scintillation proximity assay (SPA)²⁴. Briefly, each SPA reaction mixture consisted of 6 µl from the respective samples, 33.3 nM [³H]leucine (PerkinElmer) and copper chelate (His-tag) YSi beads (GE Healthcare). SPA was performed in the presence or absence of 1 × 10⁻⁵ M leucine in 20 mM Tris-HCl (pH 8.0) supplemented with NaCl and the selected amphiphile or detergent to final concentrations of 200 mM and 3.3-fold dilution of the original concentrations, respectively. In the solubilization assay, the

initial activity of LeuT was assessed by SPA performed in the presence of 0.05% DDM or 0.042% MNG-3 and leucine ($0\text{--}10^{-5}$ M, competition binding). SPA was performed with duplicate determination of all individual data points. Samples were counted in a MicroBeta liquid scintillation counter (PerkinElmer). Normalized results are expressed as mean \pm s.e.m.

R. capsulatus superassembly solubilization and stabilization assay. Specialized photosynthetic membranes from an engineered strain of *R. capsulatus*, U43[pUHTM86Bgl], lacking the LHII light-harvesting complex were used as the starting material²⁶. The isolated flash-frozen membrane aliquots from this strain were thawed, homogenized and equilibrated to 32 °C for 30 min. The amphiphiles or detergents were added at the designated concentration to 1-ml aliquots of the membranes. After incubation with the amphiphiles for 30 min at 32 °C, the solubilized material was separated from the membrane debris in an ultracentrifuge at 315,000g at 4 °C for 30 min. The supernatant was transferred into a new microcentrifuge tube containing Ni-NTA resin (Qiagen), and then the tube was incubated and inverted for 1 h at 4 °C. Once binding was complete, samples were loaded onto resin-retaining spin columns (for example, emptied His SpinTrap columns; GE Healthcare), which were then inserted into 2-ml microcentrifuge tubes. Samples were washed twice with 0.5 ml of amphiphile-containing binding buffer (a pH 7.8 Tris solution containing the amphiphile at $1\times$ CMC, 0.017 wt % above CMC, 0.2 wt % or 1.0 wt %). Finally, protein was eluted with three 0.2-liter elution buffer aliquots (this buffer was identical to binding buffer with the addition to 1 M of imidazole with same pH). Purified protein was diluted with 0.4 ml of binding buffer to reach the final sample volume to 1 ml. Small aliquots (0.2 ml) of the solutions were transferred to 0.8 ml binding buffer, and UV-visible spectra of these solutions were measured as a function of time. Degradation of the material could be monitored with the 875 nm/680 nm absorbance ratio, which decreased with time.

Stabilization and crystallization of cytochrome b_6f /MNG-3 complex. Purification of the complex cytochrome b_6f from *Chlamydomonas reinhardtii* was carried out as described in the literature²⁷ with slight modifications to exchange DDM for MNG-3. Briefly, after solubilization of thylakoid membranes with DDM and a first ion exchange chromatography in 0.4 mM DDM, the protein was loaded on a 1-ml HiTrap chelating Sepharose column (GE Healthcare), preloaded with nickel (Ni^{2+}); subsequently, the column was extensively washed with 50 ml of 0.5 mM MNG-3 in 20 mM Tris-HCl, pH 8, 250 mM NaCl and eluted with 300 mM imidazole in the same buffer. The sample was desalted on a Sephadex G-25 column (GE Healthcare) with 10 mM Tris-HCl, pH 8, 0.5 mM MNG-3 and concentrated with a Vivaspin 500 (100,000 MWCO PES) concentrator (Sartorius) from 5 to 100 μM (that is, from 0.5 to 10 mg ml^{-1}) before crystallization. All steps from purification until crystal handling were carried out at 4 °C in a cold room. Crystallization trials used the protocol involving vapor diffusion with the hanging-drop technique: the protein was mixed with an equal or half volume of reservoir solution devoid of surfactant²⁷. The crystallization strategy was adapted from conditions suitable for crystallization

with DDM. Crystals were flash frozen in liquid nitrogen, and diffraction experiments were performed at the synchrotron SOLEIL (Saint-Aubin, France) on the beamline Proxima 1. Diffraction data were integrated with XDS³⁷ and analyzed with the CCP4 package³⁸. The model was refined with PHENIX³⁹ and BUSTER⁴⁰. Plastoquinone/plastocyanine oxidoreductase activity measurements were performed according to the literature⁴¹.

Cell-free expression of proteins in the presence of amphiphiles.

Transcription and translation of genes cloned into the pEU-HIS cell-free expression vector was performed as previously reported⁴². Briefly, for each sample, a 50- μl transcription reaction containing 5 μg plasmid DNA, 80 mM HEPES, pH 7.5, 16 mM magnesium acetate, 2 mM spermidine, 10 mM dithiothreitol, 2.5 mM of each nucleotide triphosphate, 25 U RNasin (Promega) and 30 U Sp6 RNA polymerase was incubated at 37 °C for 3 h. The resultant mRNA was purified by ethanol precipitation and air-dried. The pellet was resuspended in 50 μl of the translation reaction solution, which contained dialysis buffer (30 mM HEPES, pH 7.8, 100 mM potassium acetate, 2.7 mM magnesium acetate, 1.2 mM ATP, 0.25 mM GTP, 16 mM creatine phosphate, 0.4 mM spermidine and 0.3 mM of each amino acid) supplemented with 35.6 μg creatine kinase, 24 U of RNasin and 15 μl of WEPRO 2240 (Cell Free Sciences). The reaction was transferred into a 12-kDa-MWCO dialysis cup (Cosmo Bio) suspended in a reservoir of dialysis buffer and incubated for 16 h at 26 °C. Detergents and MNG amphiphiles were added when needed at 0.1 wt % or 0.2 wt % to both the translation reaction and dialysis buffer reservoir. After overnight incubation, the 50 μl translation reaction solution was transferred to a 1.7-ml centrifuge tube and spun at 15,000 r.p.m. in an Allegra 21R centrifuge (Beckman Coulter) and F2402H rotor at 20 °C for 10 min. The supernatant was removed and added to an equal volume of $2\times$ sample buffer, while the pellet was resuspended in 100 μl $1\times$ sample buffer. After being boiled for 5 min, the samples were loaded onto an SDS-PAGE gel, electrophoresed and visualized by Coomassie staining.

34. Pourcher, T., Leclercq, S., Brandolin, G. & Leblanc, G. Melibiose permease of *Escherichia coli*: large scale purification and evidence that H^+ , Na^+ , and Li^+ sugar symport is catalyzed by a single polypeptide. *Biochemistry* **34**, 4412–4420 (1995).
35. Drew, D. *et al.* GFP-based optimization scheme for the overexpression and purification of eukaryotic membrane proteins in *Saccharomyces cerevisiae*. *Nat. Protoc.* **3**, 784–798 (2008).
36. Kawate, T. & Gouaux, E. Fluorescence-detection size-exclusion chromatography for precrystallization screening of integral membrane proteins. *Structure* **14**, 673–681 (2006).
37. Kabsch, W. Automatic processing of rotation diffraction data from crystals of initially unknown symmetry and cell constants. *J. Appl. Crystallogr.* **26**, 795–800 (1993).
38. Collaborative Computational Project. Number 4. The CCP4 Suite: Programs for Protein Crystallography. *Acta Crystallogr.* **D50**, 760–763 (1994).
39. Adams, P.D. *et al.* PHENIX: building new software for automated crystallographic structure determination. *Acta Crystallogr. D Biol. Crystallogr.* **58**, 1948–1954 (2002).
40. Bricogne, G. *et al.* BUSTER, version 2.8.0. (Global Phasing Ltd., Cambridge, UK, 2009).
41. Pierre, Y., Breyton, C., Kramers, D. & Popot, J.-L. Purification and characterization of the cytochrome b_6f complex from *Chlamydomonas reinhardtii*. *J. Biol. Chem.* **270**, 29342–29349 (1995).
42. Goren, M.A. & Fox, B.G. Wheat germ cell-free translation, purification, and assembly of a functional human stearyl-CoA desaturase complex. *Protein Expr. Purif.* **62**, 171–178 (2008).